Noble-Gas Chemistry Very Important Paper

Deutsche Ausgabe: DOI: 10.1002/ange.201607583
Internationale Ausgabe: DOI: 10.1002/anie.201607583

Syntheses and Structures of Xenon Trioxide Alkylnitrile Adducts

*James T. Goettel, Kazuhiko Matsumoto, Hélène P. A. Mercier, and Gary J. Schrobilgen**

Dedicated to Professor Karl O. Christe on the occasion of his 80th birthday

Abstract: *The potent oxidizer and highly shock-sensitive binary noble-gas oxide XeO_3 interacts with CH_3CN and CH_3CH_2CN to form $O_3XeNCCH_3$, $O_3Xe(NCCH_3)_2$, $O_3XeNCCH_2CH_3$, and $O_3Xe(NCCH_2CH_3)_2$. Their low-temperature single-crystal X-ray structures show that the xenon atoms are consistently coordinated to three donor atoms, which results in pseudo-octahedral environments around the xenon atoms. The adduct series provides the first examples of a neutral xenon oxide bound to nitrogen bases. Raman frequency shifts and Xe–N bond lengths are consistent with complex formation. Energy-minimized gas-phase geometries and vibrational frequencies were obtained for the model compounds $O_3Xe(NCCH_3)_n$ ($n = 1$–3) and $O_3Xe(NCCH_3)_n{\cdot}[O_3Xe(NCCH_3)_2]_2$ ($n = 1, 2$). Natural bond orbital (NBO), quantum theory of atoms in molecules (QTAIM), electron localization function (ELF), and molecular electrostatic potential surface (MEPS) analyses were carried out to further probe the nature of the bonding in these adducts.*

Xenon trioxide is a thermodynamically unstable and notoriously shock-sensitive solid that is formed by the hydrolysis of XeF_6 or XeF_4.[1,2] Solid XeO_3 detonates upon contact with cellulose and often spontaneously explodes above 25 °C with the release of 402 kJ mol^{-1} of energy.[3] The kinetic and thermodynamic instabilities of XeO_3 have hampered its study, particularly in the solid state. Nevertheless, the structure of XeO_3 was determined over 50 years ago by single-crystal X-ray diffraction, revealing its trigonal-pyramidal geometry (C_{3v})[1] as originally predicted by the VSEPR model of molecular geometry.[4] Raman spectroscopy also confirmed the presence of XeO_3 (C_{3v} symmetry) in its concentrated aqueous solutions, whereas xenic acid, H_2XeO_4, was not observed but presumed to be present in trace amounts.[5] The IR spectrum of solid XeO_3 has also been reported.[6] The majority of studies related to XeO_3 have focused on its oxidizing properties in aqueous solutions.[7–9] Xenon trioxide has also been shown to behave as a F^- [10] and Cl^- [11] acceptor, and there is preliminary evidence for the interaction of XeO_3 with Br^-.[11] Aside from the crystal structure of solid XeO_3,[1] the only crystal structures reported that contain the XeO_3 moiety are those of $K[FXeO_3]$[12] and $M_9(XeO_3Cl_2)_4Cl$[13] (M = Cs, Rb); however, the chloro-anion structures were disordered.

The choice of compatible ligands and solvents for XeO_3 is limited by its strong oxidant properties. For example, XeO_3 rapidly oxidizes primary and secondary alcohols to CO_2 and H_2O.[14] However, CH_3CN is relatively resistant to oxidation by xenon fluorides and xenon oxide fluorides.[15,16] The ^{129}Xe NMR spectrum of XeO_3 in water was reported in 1974.[17] Complexes between XeF_6 and CH_3CN were recently synthesized and characterized, providing the first evidence for the formation of Xe^{VI}–N bonds.[16]

Herein, the syntheses and characterization of four alkylnitrile adducts of XeO_3, namely $O_3XeNCCH_3$ (**1**), $O_3Xe(NCCH_3)_2$ (**2**), $O_3XeNCCH_2CH_3$ (**3**), and $O_3Xe(NCCH_2CH_3)_2$ (**4**), are reported. Preliminary findings related to **1** and **2** were recently presented.[18] Pure XeO_3 was synthesized by hydrolysis of XeF_6 with three equivalents of water [Eq. (1)] in

$$XeF_6 + 3\,H_2O \rightarrow XeO_3 + 6\,HF \qquad (1)$$

Freon 114 (1,2-dichlorotetrafluoroethane) followed by removal of HF and the solvent under dynamic vacuum between −78 and 0 °C. Acetonitrile was then added to XeO_3 to form $O_3Xe(NCCH_3)_2$ (**2**). Handling of pure XeO_3 without detonation proved to be difficult. A safer, more convenient, and reliable method was to initially hydrolyze XeF_6 in CH_3CN solvent at 0 °C. Slow cooling of this solution led to the formation of large block-shaped crystals, which were shown to be **2** by low-temperature X-ray crystallography.

The $O_3XeNCCH_3$ adduct (**1**) was initially synthesized by the reaction of XeO_4 with CH_3CN at −40 °C according to Eq. (2). As yellow XeO_4 decomposed, large, colorless plates

$$XeO_4 + CH_3CN \rightarrow O_3XeNCCH_3 + {}^1\!/_2\,O_2 \qquad (2)$$

crystallized, which proved to be exceedingly shock-sensitive. An alternative synthesis involving CH_3CN displacement from **2** in anhydrous HF (aHF) also afforded **1** and $CH_3CN{\cdot}(HF)_x$ [Eq. (3)].

$$O_3Xe(NCCH_3)_2 + x\,HF \rightarrow O_3XeNCCH_3 + CH_3CN \cdot (HF)_x \qquad (3)$$

Both **3** and **4** can be synthesized by direct reaction of XeO_3 in CH_3CH_2CN solvent [Eq. (4)] and by varying the

$$XeO_3 + n\,CH_3CH_2CN \rightarrow O_3Xe(NCCH_2CH_3)_n \quad (n = 1, 2) \qquad (4)$$

concentration of XeO_3, that is, the 1:2 adduct, **4**, is formed at lower temperatures and concentrations whereas the 1:1

[*] J. T. Goettel, Dr. K. Matsumoto, Dr. H. P. A. Mercier, Prof. G. J. Schrobilgen
Department of Chemistry, McMaster University
Hamilton, ON L8S 4M1 (Canada)
E-mail: schrobil@mcmaster.ca

Supporting information and the ORCID identification number(s) for the author(s) of this article can be found under: http://dx.doi.org/10.1002/anie.201607583.

adduct, **3**, is formed at higher temperatures in more concentrated solutions.

Thus far, attempts to isolate $O_3Xe(NCCH_3)_3$ and $O_3Xe(NCCH_2CH_3)_3$ by use of other solvents, such as SO_2ClF, aHF, and Freon 114, at low temperatures have proven unsuccessful.

The $O_3XeNCCH_3$ adduct (**1**) is a thermodynamically unstable, extremely shock-sensitive material that requires very careful handling. In marked contrast, crystalline $O_3Xe(NCCH_3)_2$ (**2**) appears to be insensitive to mechanical shock and is kinetically stable at room temperature, but slowly loses CH_3CN in air. Crystalline samples did not detonate when struck with a hammer, but detonated on contact with cellulose. Samples of **2** lost CH_3CN when left under dynamic vacuum at −15 °C, which resulted in the formation of highly shock-sensitive **1**.

Data collection details and other crystallographic information pertaining to **1**–**4** are provided in Table 1 and in the Supporting Information, Table S1. Selected bond lengths and angles are provided in Table 2 and a full list of geometrical parameters is given in Table S2.

Table 2: Selected bond lengths [Å] and angles [°] of adducts **1**–**4**.

	1	**2**	**3**	**4**
Xe---N	2.766(2)	2.8088(11) 2.8062(10)	2.778(3)	2.8560(8) 2.8186(9)
Xe−O	1.7709(11) 1.7532(15)	1.7710(8) 1.7583(8) 1.7556(8)	1.763(2) 1.753(3) 1.756(2)	1.7694(6) 1.7597(9) 1.7561(7)
Xe---O	2.7209(11)	2.7578(8)	2.761(2) 2.755(3)	2.8348(6)
N-Xe-O	166.05(8)	162.43(4) 160.92(4)	162.5(1)	161.93(3)
Xe-N-C	154.69(19)	138.80(10) 154.61(10)	146.6(2)	156.94(7) 157.97(7)

Table 1: Data collection details and other crystallographic information.

Chemical formula	$O_3XeNCCH_3$ (**1**)	$O_3Xe(NCCH_3)_2$ (**2**)	$O_3XeNCCH_2CH_3$ (**3**)	$O_3Xe(NCCH_2CH_3)_2$ (**4**)
space group	*Pmna*	$P2_1/c$	*Pbcn*	$P2_1/n$
a [Å]	14.9904(4)	8.5098(5)	16.6092(3)	7.9753(7)
b [Å]	6.3364(2)	12.6371(8)	8.6901(1)	8.8063(7)
c [Å]	5.56880(10)	8.5727(5)	17.3961(3)	14.1568(12)
β [°]	90	118.849(2)	90	93.486(4)
V [$Å^3$]	528.95(2)	807.49(8)	2510.88(7)	992.43(14)
Z	4	4	16	4
M_w [$g\,mol^{-1}$]	220.35	261.41	234.38	289.45
ρ_{calcd} [$g\,cm^{-3}$]	2.767	2.150	2.480	1.937
T [°C]	−173	−173	−173	−173
μ [mm^{-1}]	6.414	4.224	5.413	3.447
R_1[a]	0.0222	0.0177	0.0262	0.0186
wR_2[b]	0.0463	0.0299	0.0603	0.0472

[a] R_1 is defined as $\Sigma||F_o|-|F_c||/\Sigma|F_o|$ for $I>2\sigma(I)$. [b] wR_2 is defined as $[\Sigma[w(F_o^2-F_c^2)^2]/\Sigma w(F_o^2)^2]^{1/2}$ for $I>2\sigma(I)$.

The crystal structure of $O_3XeNCCH$ (**1**; Figures 1 a and S1 a) contains layers of trigonal-pyramidal XeO_3 molecules separated by CH_3CN layers. Aside from its primary Xe−O bonds, each xenon atom has one Xe---N bond (2.766(2) Å) to CH_3CN and two equivalent Xe---O contacts (2.721(1) Å) with two different neighboring XeO_3 molecules. The Xe---N bond length does not significantly differ from those of $F_6XeNCCH_3$ (2.762(2) Å) but is slightly shorter than those of $F_6Xe(NCCH_3)_2{\cdot}CH_3CN$ (2.785(2) Å). The primary Xe−O bonds *trans* to the Xe---O contacts (1.7709(11) Å) are significantly longer than the Xe−O bonds *trans* to nitrogen (1.7532(15) Å). The O atoms of the longer Xe−O bonds have contacts to the Xe atoms of adjacent XeO_3 molecules, whereas the O atoms of the shorter Xe−O bonds have no significant contacts. Structure **3** (Figures 1 b and S2 a) also contains alternating XeO_3 and CH_3CH_2CN layers (Figure S2 a). The Xe---N bond (2.778(3) Å) of **3** is longer, but otherwise, the adduct geometry is very similar to that of its CH_3CN analogue.

The crystal structure of $O_3Xe(NCCH_3)_2$ (**2**; Figures 1 c and S1 b) consists of chains that are well isolated from one another. The Xe atom of each XeO_3 molecule has one Xe---O contact and two Xe---N bonds with two different CH_3CN molecules. Similar to **1**, the Xe−O bridge bond (1.7710(8) Å) is elongated relative to the other two primary terminal Xe−O bonds (1.7583(8), 1.7556(8) Å). The Xe---N bonds (2.806(1), 2.809(1) Å) are significantly longer than those of **1** (2.766(2) Å) because additional electron density is donated to the Xe atoms from the

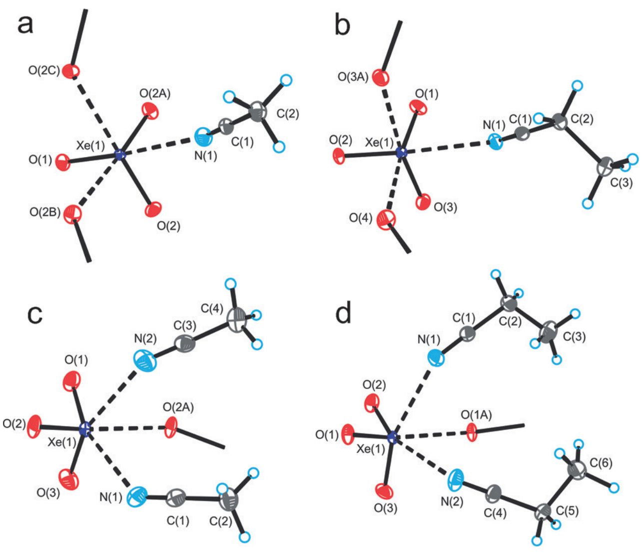

Figure 1. The X-ray crystal structures of a) $O_3XeNCCH_3$ (**1**) (*Pmna*), b) $O_3Xe(NCCH_3)_2$ (**2**) ($P2_1/c$), c) $O_3XeNCCH_2CH_3$ (**3**) (*Pbcn*), and d) $O_3Xe(NCCH_2CH_3)_2$ (**4**; $P2_1/n$) at −173 °C. Thermal ellipsoids set at 50 % probability.

second CH_3CN ligand. The structure of **4** (Figures 1d and S2b) displays longer
Xe---N bonds (2.8186(9), 2.8560(8) Å).

The bond lengths and angles are similar to those of solid XeO_3, which is likely a consequence of the large uncertainties associated with the previously reported crystal structure of XeO_3.[1] The N---Xe-O angles of the CH_3CH_2CN adducts are smaller than those of the CH_3CN adducts, ranging from 161.93(3)° (**4**) to 166.05(8)° (**1**).

The low-temperature Raman spectra of **1–4** are depicted in Figures S3–S6. Because of their extreme shock sensitivities and the possibility that the isolated dry solid could detonate during spectral acquisition, the Raman spectrum of **1** was obtained from the crystalline solid under a dilute solution of CH_3CN in aHF at −80°C. The room-temperature Raman spectrum of aqueous XeO_3 features four bands (Table S3) at 317 (E, δ_{asym}), 344 (A_1, $\delta_{umbrella}$), 780 (A_1, ν_{sym}), and 833 cm^{-1} (E, ν_{asym}),[4] whereas the room-temperature Raman spectrum of XeO_3 in CH_3CN displays four similar XeO_3 bands at 307, 339, 782, and 846 cm^{-1}, respectively. The most intense bands ($\nu(XeO_3)_{sym}$) of **1** and **2** (Table S4) as well as **3** and **4** (Table S5) have very similar frequencies, occurring at 762 cm^{-1} and 770/771 cm^{-1}, respectively. The C≡N stretching bands are shifted to higher frequencies relative to those of solid (−150°C) CH_3CN (2248 cm^{-1}) and CH_3CH_2CN (2247 cm^{-1}). Such high-frequency ligand complexation shifts are consistent with adduct formation: see $F_6XeNCCH_3$ (2266.2 cm^{-1}),[16] $F_6Xe(NCCH_3)_2{\cdot}CH_3CN$ (2271.5 cm^{-1}),[16] and $F_2OXeNCCH_3$ (2254.2 cm^{-1}).[15]

The bonding in these adducts was explored by DFT calculations at the B3LYP/Def2-SVPD(H,C,N,O)/aug-cc-pVTZ-PP(Xe) level of theory. Although a recent computational study attempted to model the gas-phase interaction between CH_3CN and XeO_3, the resulting geometries do not agree with the present experimental and calculated geometries, nor do they account for the extended structures of these complexes in the solid state (see the Supporting Information).[19] The NBO analyses (Tables S6 and S7) show that the N lone pairs of the bases are sp-hybridized and are the electron donor orbitals. The N lone pairs are delocalized (0.61–0.74%) into the σ^*_{Xe-O} LUMO, resulting in interaction energies ranging from 11.8 to 12.1 kJ mol^{-1}. Contrary to the previously reported model,[19] there is essentially no interaction between the π system of the C≡N triple bond and XeO_3. The side-on coordination of CH_3CN is likely favored in the gas phase owing to weak CH···O intramolecular hydrogen-bonding interactions that the authors of the previous study did not comment on.[19] Similar interactions also occur between adjacent layers in the solid state. The nature of the Xe---N and Xe−O bonding was also investigated by the quantum theory of atoms in molecules (QTAIM) analyses. Both the N and Xe valence electron lone pairs (VELPs) are readily discernable in the contour (Figure S10) and relief maps (Figure S11). The Xe−O Laplacian of electron density ($\nabla^2\rho_b$) decreases (0.295 to 0.285) upon coordination of multiple CH_3CN ligands, whereas the C≡N $\nabla^2\rho_b$ increases (0.409 to 0.761; Table S8). Electron localization function (ELF) analyses were also carried out to visualize and compare the behavior of the Xe VELPs. The ELF isosurface plots (Figure S8) show that the Xe VELP of XeO_3 is asymmetrically distorted upon adduct formation with one or two ligands, but remains symmetric, although flattened, when Xe is coordinated to three ligands. The most positive electrostatic potentials (EPs) on the MEPS of XeO_3 (+251 kJ mol^{-1}; Figure S13) are located on Xe *trans* to the Xe=O bonds and correspond to σ holes. In contrast, the maximum EP at the Xe VELP is significantly smaller (+234 kJ mol^{-1}). The N VELPs avoid the Xe VELP, coordinating into regions of high electrostatic potential that are on Xe, at the periphery of the Xe VELP. This results in N trajectories that are essentially *trans* to O ligands. The above analyses show that the Xe---N bonds have very low covalent character and are primarily electrostatic and can be described as σ-hole bonds.

In conclusion, the first XeO_3 nitrogen base adducts, **1–4**, have been synthesized and characterized by low-temperature Raman spectroscopy and X-ray crystallography. The Xe---N bonds are primarily electrostatic in nature and can be described in terms of interactions of the N VELPs with Xe σ holes. Although 1:3 adducts could not be obtained, the use of stronger nitrogen bases is expected to lead to 1:3 adducts in which the XeO_3 molecules are well isolated from one another and possibly less shock-sensitive. The amphoteric Lewis acid/base nature of XeO_3 is key to the bonding and extended structures of these adducts. Further investigations of the coordination chemistry of XeO_3 are currently in progress.

Experimental Section

Caution! Solid XeO_3 is an extremely shock-sensitive, highly energetic compound. Every effort should be made to avoid formation of the solid. Reaction vessels made of glass should be avoided, and appropriate protective equipment should be used (see the Supporting Information).

Synthesis of **1**: Xenon tetroxide was synthesized from Na_4XeO_6 and 100% H_2SO_4 as previously described (see the Supporting Information).[20] Xenon tetroxide (ca. 15 mg) was condensed under static vacuum at −196°C onto the walls of an FEP reaction tube (0.64 cm outer diameter, 0.48 cm inner diameter) containing CH_3CN (156 mg, 0.123 mL). Upon warming the reaction mixture to −40°C, XeO_4 dissolved in CH_3CN forming a colorless solution. Large colorless plates crystallized over the next several hours. For an alternative synthesis, see the Supporting Information.

Synthesis of **2**: Xenon hexafluoride (28.4 mg, 0.116 mmol) was transferred under static vacuum at −196°C. Freon 114 (ca. 0.1 mL) was condensed onto XeF_6 at −196°C followed by condensation of CH_3CN onto the upper walls of the reactor at −196°C. The reactor was allowed to warm to −40°C, and the contents were carefully mixed to allow XeF_6 to diffuse into the upper CH_3CN layer. Three equivalents of H_2O (6.3 mg, 0.35 mmol) were added to the reactor at 0°C by use of a microsyringe. The reactor was warmed to 20°C, and the mixture was thoroughly mixed. Cooling the reactor to 0°C resulted in the formation of large, colorless, rod-shaped crystals, which continued to grow as the temperature was slowly decreased to −40°C. Acetonitrile and HF were removed under dynamic vacuum between −40 and −30°C.

The syntheses of **3** and **4** are described in the Supporting Information. Details that relate to the synthetic work, Raman spectroscopy, low-temperature crystal mounting, X-ray data collection, and X-ray structure refinement are also provided in the Supporting Information.

CCDC 1497743 (**1**), 1497744 (**3**), 1497745 (**2**), and 1497746 (**4**) contain the supplementary crystallographic data for this paper. These data can be obtained free of charge from The Cambridge Crystallographic Data Centre.

Acknowledgements

We thank the Natural Sciences and Engineering Research Council of Canada (NSERC) for support in the form of a Discovery Grant (G.J.S.) and a CGS-D scholarship (J.T.G.). We are also grateful for the computational resources provided by SHARCNet (Shared Hierarchical Academic Research Computing Network, www.sharcnet.ca).

Keywords: fluorine chemistry · noble-gas chemistry · Raman spectroscopy · xenon oxides · X-ray crystallography

How to cite: *Angew. Chem. Int. Ed.* **2016**, *55*, 13780–13783
Angew. Chem. **2016**, *128*, 13984–13987

[1] D. F. Smith, *J. Am. Chem. Soc.* **1963**, *85*, 816–817.
[2] D. H. Templeton, A. Zalkin, J. D. Forrester, S. M. Williamson, *J. Am. Chem. Soc.* **1963**, *85*, 817.
[3] S. R. Gunn in *Noble-Gas Compounds* (Ed.: H. H. Hyman), University of Chicago Press, Chicago, IL, **1963**, pp. 149–151.
[4] R. J. Gillespie in *Noble-Gas Compounds* (Ed.: H. H. Hyman), University of Chicago Press, Chicago, IL, **1963**, pp. 333–339.
[5] H. H. Claassen, G. Knapp, *J. Am. Chem. Soc.* **1964**, *86*, 2341–2342.
[6] B. Jaselskis, T. M. Spittler, *J. Am. Chem. Soc.* **1965**, *85*, 3357–3360.
[7] B. Jaselskis, J. P. Warriner, *Anal. Chem.* **1966**, *38*, 563–564.
[8] S. A. Shackelford, G. U. Yuen, *Inorg. Nucl. Chem. Lett.* **1973**, *9*, 605–609.
[9] L. A. Khamidullina, S. V. Lotnik, V. P. Kazakov, *Kinet. Catal.* **2008**, *49*, 27–33.
[10] B. Jaselskis, J. L. Huston, *J. Am. Chem. Soc.* **1969**, *91*, 1874–1875.
[11] P. LaBonville, J. R. Ferraro, T. M. Spittler, *J. Chem. Phys.* **1971**, *55*, 631–640.
[12] D. Hodgson, J. A. Ibers, *Inorg. Chem.* **1969**, *8*, 326–331.
[13] R. D. Willett, S. W. Peterson, B. A. Coyle, *J. Am. Chem. Soc.* **1977**, *99*, 8202–8207.
[14] B. Jaselskis, *Rec. Chem. Prog.* **1970**, *31*, 103–132.
[15] D. S. Brock, V. Bilir, H. P. A. Mercier, G. J. Schrobilgen, *J. Am. Chem. Soc.* **2007**, *129*, 3598–3611.
[16] K. Matsumoto, J. Haner, H. P. A. Mercier, G. J. Schrobilgen, *Angew. Chem. Int. Ed.* **2015**, *54*, 14169–14173; *Angew. Chem.* **2015**, *127*, 14375–14379.
[17] K. Seppelt, H. H. Rupp, *Z. Anorg. Allg. Chem.* **1974**, *409*, 331.
[18] J. T. Goettel, G. J. Schrobilgen, *Abstracts of Papers.* Chemistry and structures of xenon(VIII) compounds. Presented at the 248th ACS National Meeting and Exposition, San Francisco, USA, August 10–14, **2014**, Poster No. 56.
[19] A. Bauzá, A. Frontera, *Angew. Chem. Int. Ed.* **2015**, *54*, 7340–7343; *Angew. Chem.* **2015**, *127*, 7448–7451.
[20] M. Gerken, G. J. Schrobilgen, *Inorg. Chem.* **2002**, *41*, 198–204.

Received: August 4, 2016
Revised: August 29, 2016
Published online: September 30, 2016